Changes in Microstructure of Biomedical Co-Cr-Mo Alloys during Aging at 973 to 1373 K

doi: 10.2320/matertrans.MI201507

Materials Transactions, Vol. 57, No. 12 (2016) pp. 2048 to 2053
Special Issue on Advances in Biomedical Materials Science and Technology

Changes in Microstructure of Biomedical Co-Cr-Mo Alloys during Aging at 973 to 1373 K

Kosuke Ueki[1], Yuto Kurihara[1,*1], Shingo Mineta[1,*2], Alfirano[2], Kyosuke Ueda[1], Shigenobu Namba[3], Takashi Yoneda[4] and Takayuki Narushima[1,*3]

[1]*Department of Materials Processing, Tohoku University, Sendai 980–8579, Japan*
[2]*Metallurgy Engineering Department, Sultan Ageng Tirtayasa University, Cilegon, 42435, Indonesia*
[3]*Materials Research Laboratory, Kobe Steel, Ltd., Kobe 651–2271, Japan*
[4]*Yoneda Advanced Casting Co., Ltd., Takaoka 933–0951, Japan*

Changes in the microstructure and hardness of biomedical Co-Cr-Mo forged alloys (Co-27Cr-6Mo-0.77Si-0.64Mn-0.17N-0.06C (mass%)) during aging were investigated with a focus on precipitation. After solution treatment at 1523 K for 1.8 ks, the alloys were subjected to aging at temperatures between 973 and 1373 K for up to 86.4 ks. η-phase (M_6X-$M_{12}X$ type), $M_{23}X_6$-type and π-phase (A_2T_3X type) precipitates were detected after aging. The formation of π-phase precipitates was detected in alloys aged between 1023 and 1123 K for holding times $\geq$ 21.6 ks, with a nose temperature between 1073 and 1123 K. The presence of π-phase precipitates in the aged Co-Cr-Mo alloy is reported for the first time; N contained within the alloy is believed to contribute to formation of the π-phase. The formation of a hexagonal-close-packed Co-based metallic phase (ε-phase) was observed between 1023 and 1123 K. The Vickers hardness increased in alloys aged at 1023 and 1073 K. This increase in hardness is attributed to the presence of π-phase and ε-phase and their wide-area precipitation. [doi:10.2320/matertrans.MI201507]

(Received April 21, 2016; Accepted July 15, 2016; Published August 26, 2016)

Keywords: *cobalt-chromium alloy, precipitate, hardness, aging, microstructure, biomaterials*

1. Introduction

Biomedical Co-Cr-Mo alloys have been registered in ASTM F75, F799 and F1537 standards, and applied as materials for artificial joints and denture bases because of their excellent mechanical, wear and corrosive properties[1–3]. Precipitation in Co-Cr-Mo alloys is known to be closely related to their properties such as mechanical strength[4,5] and wear resistance[6–8]. We have previously studied the formation and dissolution of precipitates in Co-Cr-Mo alloys during heat treatment at temperatures above 1400 K[9–14]. Intermetallics such as σ-phase (Co(Cr,Mo)) and χ-phase with α-Mn structure and carbonitrides such as M_2X-type (where M is a metallic element and X is C and/or N), M_7X_3-type, $M_{23}X_6$-type, π-phase (A_2T_3X type, where A and T are metallic elements with low and high affinity with X) and η-phase (M_6X-$M_{12}X$ type) have all been detected as precipitates in Co-Cr-Mo alloys[15].

The precipitation behavior of Co-Cr-Mo-C alloys during aging at lower temperatures has been reported[16–19], with $M_{23}X_6$-type[16–19], η-phase[16] and σ-phase[16] precipitates being detected. The addition of N is effective in improving the workability[20,21] and mechanical strength[22,23] of Co-Cr-Mo alloys. Kurosu *et al.*[24] reported microstructural changes in a Co-Cr-Mo alloy containing 0.16 mass% N and 0.04 mass% C during heat treatment at 1073 K. They reported the formation of a hexagonal-close-packed (hcp) Co-base metallic phase (ε-phase) and Cr_2N from a face-centered-cubic (fcc) Co-base metallic phase (γ-phase). Despite all these previous studies, the precipitation behavior of Co-Cr-Mo-N-C alloys during aging at low temperatures is not fully understood. In this study, changes in microstructure and hardness of a biomedical Co-Cr-Mo alloy with added N and C were investigated during aging over a wide temperature range (973–1373 K).

2. Experimental Procedures

In this study, a biomedical Co-27Cr-6Mo forged alloy bar (33 mm diameter) with a chemical composition as listed in Table 1 was used. The N and C contents within the alloy were 0.17 and 0.06 mass%, respectively. The C content of 0.06 mass% is enough to form carbide-based precipitates such as the $M_{23}X_6$-type[25]. The bar was cut into disks 5 mm thick. Specimens for heat treatment were prepared by dividing each disk into six equal parts, in the pattern depicted in Fig. 1. Before aging, the specimens were solution-treated at 1523 K for 1.8 or 43.2 ks to completely dissolve any precipitates present in the forged alloy into the metallic matrix. Aging was conducted at temperatures between 973 and 1373 K with holding times of 0.9 to 86.4 ks. Specimens were placed

Table 1 Chemical composition of the alloy used in this study (mass%).

Cr	Mo	C	N	Si	Mn	Co
27	6	0.06	0.17	0.77	0.64	Bal.

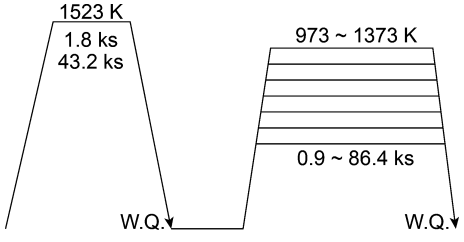

Fig. 1 Schematic drawing of the heat treatment pattern.

*1Present address: Nippon Micrometal Co., Iruma 358–0032, Japan
*2Present address: NTT Device Technology Laboratories, Atsugi 243–0198, Japan
*3Corresponding author, E-mail: narut@material.tohoku.ac.jp

in sealed SiO_2 ampoules for both the solution treatment and aging. The atmosphere inside the SiO_2 ampoule was Ar at a pressure of approximately 0.02 MPa at room temperature. The SiO_2 ampoules containing the alloy specimens were placed into an electric resistance muffle furnace maintained at a fixed temperature. After heat treatment, the specimens were water-quenched with breaking the ampoules.

The solution-treated and aged alloys were cut along the thickness dimension, and the cross section was wet-polished with emery papers (up to a 1500 grit size) and buff-polished with a diamond paste (1-μm grain size). Some of the polished specimens were electrolytically etched at 6 V in a 10% H_2SO_4-methanol solution. The microstructures of the alloy specimens were observed using an optical microscope (OM, BX60M, Olympus, Tokyo, Japan) and a scanning electron microscope (SEM, XL30FEG, Philips, Hillsboro, OR). The precipitates in the aged specimens were electrolytically extracted at room temperature in a 10% H_2SO_4 aqueous solution at 2 V after removal of surface oxides by mechanical polishing. Pt was used for electrodes, while the alloy specimens were held by Pt wire. Precipitates can be extracted because the metallic matrix of the specimen dissolves into the electrolyte solution. The extracted precipitates were collected as the residue after filtration and washed with ultrapure water. The phase of the extracted precipitates was identified using X-ray diffraction (XRD, D8 ADVANCE, Bruker AXS, Karlsruhe, Germany) with Cu Kα radiation[9]. The morphologies of the extracted precipitates were observed using SEM. The combination of electrolytic extraction, XRD and SEM allows for direct and precise analysis of the phase and morphology of precipitates.

In order to study the phase of the metallic matrix, the ε-phase fraction (f^{hcp}) in the solution-treated and aged alloys was evaluated using eq. (1).

$$f^{hcp} = I_{101}{}^{hcp}/(I_{101}{}^{hcp} + 1.5I_{200}{}^{fcc}) \quad (1)$$

where $I_{101}{}^{hcp}$ and $I_{200}{}^{fcc}$ are peak intensities of the hcp ε-phase (101) and fcc γ-phase (200), respectively. This equation, first proposed by Sage and Guillaud[26], is based on the peak intensities of the ε-phase and γ-phase in the XRD patterns. Prior to XRD measurement, the deformed parts of the alloy specimens, formed by mechanical polishing, were removed by electrolytic polishing.

Changes in alloy hardness after aging were evaluated using a micro Vickers hardness tester (HM-102, Mitsutoyo, Tokyo, Japan) with a load of 1 kgf. The reported hardness is the mean value of seven individual measurements.

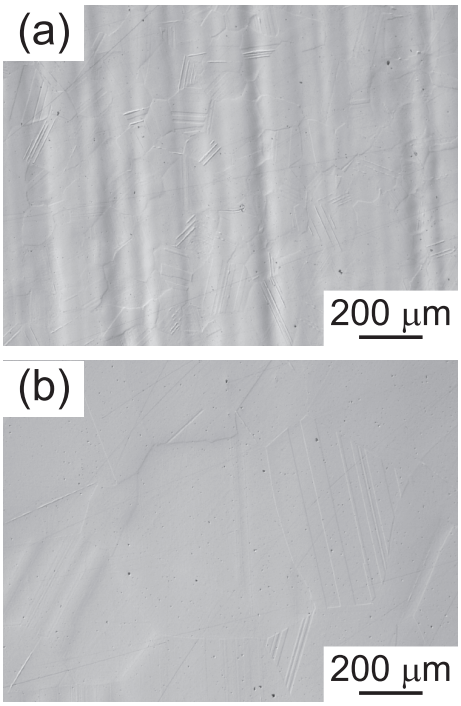

Fig. 2 OM images of the microstructure of the alloys after solution treatment at 1523 K for (a) 1.8 and (b) 43.2 ks.

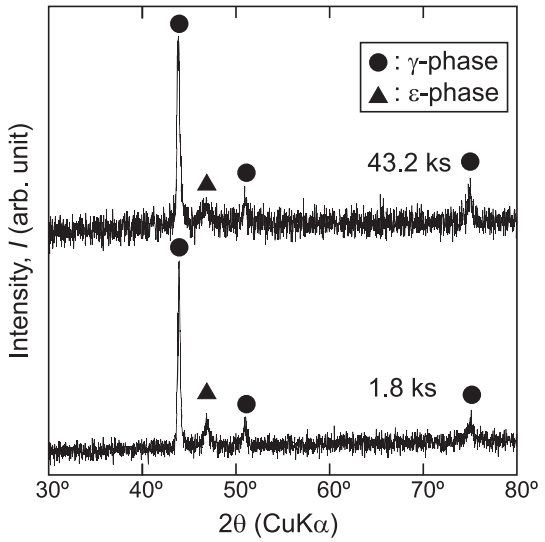

Fig. 3 XRD patterns of the alloys after solution treatment at 1523 K for 1.8 and 43.2 ks.

3. Results and Discussion

OM images showing the microstructures of the solution-treated alloys can be found in Fig. 2. The precipitates in the forged alloy were completely dissolved into the metallic matrix, and no precipitates were observed even after 1.8 ks of solution treatment. Therefore, solution treatment before aging was conducted at 1523 K for 1.8 ks for further studies. The alloy grain size was around 120 μm. Both the major γ-phase and minor ε-phase were detected in the XRD patterns of the metallic matrix after solution treatment (Fig. 3). The change in the ε-phase fraction with solution treatment time was insignificant, indicating that the ε-phase detected by XRD is formed by a martensitic transformation during quenching after the solution treatment.

Figure 4 shows the microstructures of the alloys after aging at 973, 1023, 1073, 1123 and 1223 K. When aged at 973 K for 0.9 ks, precipitates were not observed, and the microstructure was similar to that of the solution-treated alloy. Precipitation was detected at the grain boundary after aging for 86.4 ks. When aged at 1023 K for 86.4 ks, precipitates were found to grow over a wide area from the grain boundary to intragrain regions. Marked precipitation occurred when aged

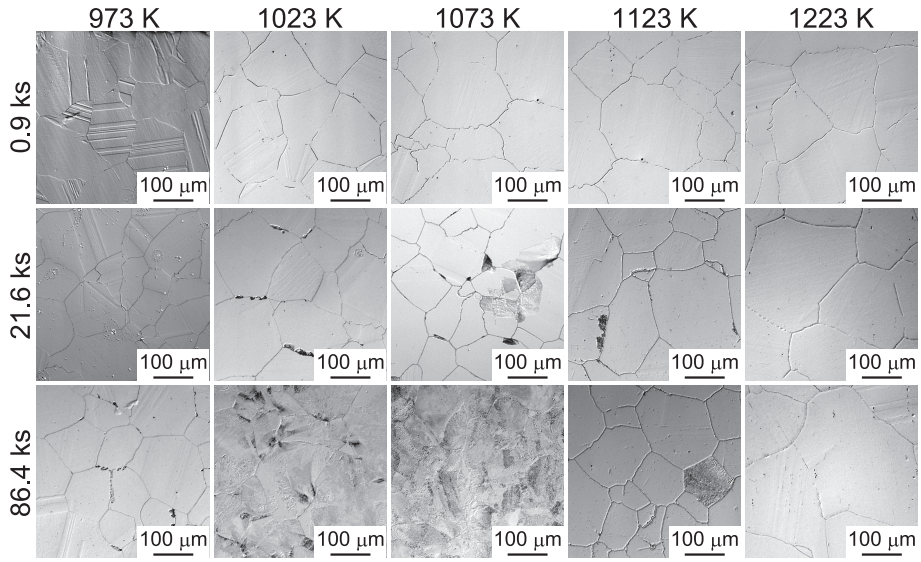

Fig. 4 SEM images of the microstructure of the alloys aged at 973, 1023, 1073, 1123 and 1223 K.

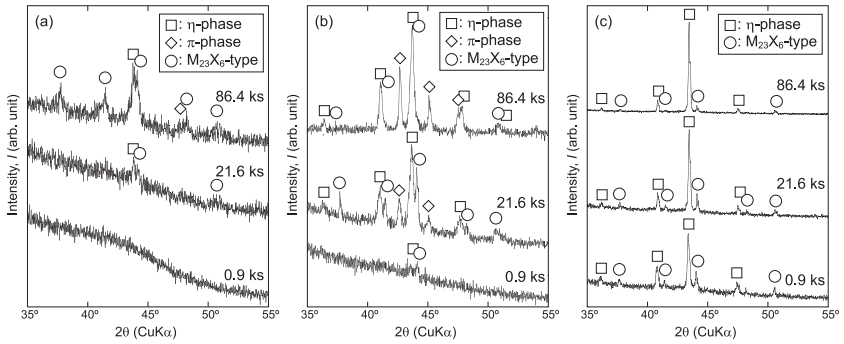

Fig. 5 XRD patterns of the precipitates electrolytically extracted from the alloys aged at (a) 973, (b) 1073 and (c) 1223 K.

at 1073 K, and precipitated microstructures were found to cover almost the entire area after aging for 86.4 ks. At 1123 K, precipitates were found to spread to intragrain regions in some grains, but precipitation was not extensive. At 1223 K, precipitation occurred primarily at the grain boundaries.

XRD patterns of the precipitates obtained by electrolytic extraction of the aged alloys are shown in Fig. 5. The η-phase and $M_{23}X_6$-type precipitates were observed at 973 and 1223 K, while the formation of π-phase precipitates as well as η-phase and $M_{23}X_6$-type precipitates was confirmed at 1073 K.

The precipitate phases in the aged alloys are summarized in Fig. 6 using a time-temperature-precipitation (TTP) diagram. Each point in the figure corresponds to the phases present, listed from left to right in order of decreasing content. The precipitate ratios were assumed to be the same as the intensity ratios of the strongest peak for each precipitate in the XRD patterns[14,27]. No precipitates were detected using XRD for alloys aged at 973 and 1023 K for short holding times, and at 1373 K for all holding times. For all conditions where precipitates were detected, the η-phase was the most common precipitate. η-phase and $M_{23}X_6$-type precipitates were observed in temperature ranges of 973 to 1323 K and 973 to 1223 K, respectively. These precipitates were detected for wide temperature ranges even after aging at the shortest holding time (0.9 ks). Therefore, a nose temperature could not be determined in the TTP diagram. The formation of π-phase precipitates was detected in alloys aged between 1023 and

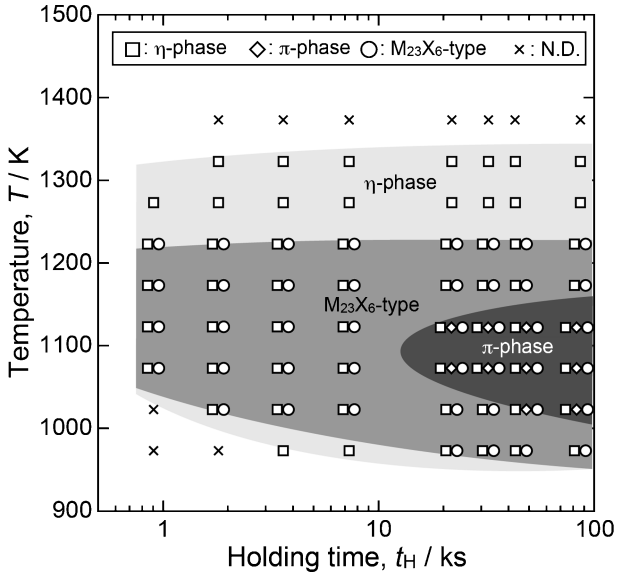

Fig. 6 Precipitate phases in the aged alloys. N.D. means no precipitates were detected in XRD analysis.

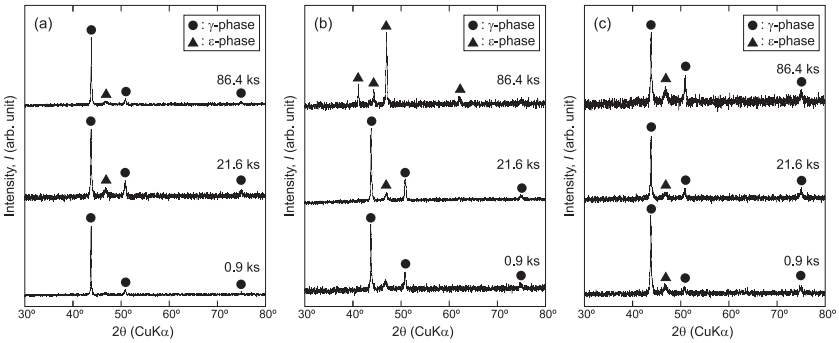

Fig. 7 XRD patterns of the metallic matrix of the alloys aged at (a) 973, (b) 1073 and (c) 1223 K.

1123 K for holding times ≥ 21.6 ks, with a nose temperature between 1073 and 1123 K. We previously reported the formation of π-phase precipitates in Co-Cr-Mo alloys during heat treatment at high temperatures, where liquid and solid phases coexist[9,12,15]. The formation of π-phase precipitates during aging of Co-Cr-Mo alloy systems at low temperatures has not previously been reported. The formation of intermetallic σ-phase precipitates during aging was reported in Co-Cr-Mo alloys without the addition of N and C[28,29]. The addition of N has been shown to stabilize η-phase and π-phase precipitates[15] while suppressing σ-phase formation[13]. In our case, η-phase and π-phase precipitation was observed in the present alloy with 0.17 mass% of N.

Kurosu *et al.* found that Cr_2N precipitates formed in Co-27.2Cr-5.5Mo-0.16N-0.04C alloys during aging at 1073 K for 90 ks[24]. The N and C contents and aging condition used by Kurosu *et al.* are similar to those in this study; however, the precipitate phases were altered by the presence of 1 mass%-Si or 1 mass%-Mn[30]. One possible explanation for this is that different amounts of minor alloying elements such as Si and Mn changed the phase of the precipitates, although the exact amount of Si and Mn are not mentioned in the study (Ref. 24)).

Figure 7 shows the XRD patterns of the metallic matrix of alloys aged at 973, 1073 and 1223 K. A weak ε-phase peak was detected at 973 and 1223 K; however, the peak intensity did not increase with increasing holding times, and was similar to the intensity of the peak after solution treatment (Fig. 3). This suggests that the ε-phase was formed by a martensitic transformation during quenching after, not during, isothermal aging. On the other hand, at 1073 K, a marked increase in the ε-phase fraction was detected and a single ε-phase was formed after aging for 86.4 ks. The formation region of the ε-phase is summarized in Fig. 8. In this region, the ε-phase fraction (f^{hcp}) after aging was 0.1 higher than after solution treatment. The formation of the ε-phase was observed between 1023 and 1123 K for holding times ≥ 32.4 ks, with a nose temperature at approximately 1073 K. The formation of an ε-phase during aging has been previously reported for cast[31] and wrought[29,32] Co-Cr-Mo alloys. These reports demonstrate C-shaped curves with a nose temperature between 1023 and 1123 K for ε-phase formation, which matches the present results.

Changes in Vickers hardness as a function of aging holding time are summarized in Fig. 9. The hardness of the solution-treated alloy was 328 Hv, and was shown to increase after aging at 1023 and 1073 K, reaching 492 and 539 Hv, respectively. No marked increase in hardness was detected at the other aging temperatures, compared to after solution treatment. The morphologies of the precipitates electrolytically extracted from the alloys aged at 1023, 1073 and 1123 K for 86.4 ks are shown in Fig. 10. The precipitates formed at

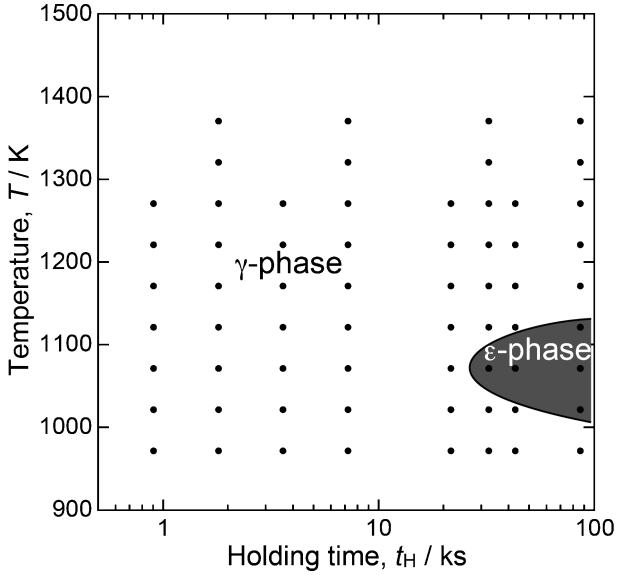

Fig. 8 Formation region of γ-phase in the aged alloys.

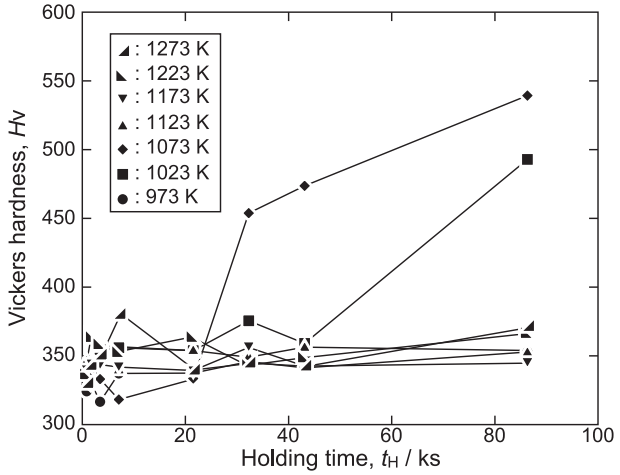

Fig. 9 Change in Vickers hardness with holding time in the aged alloys.

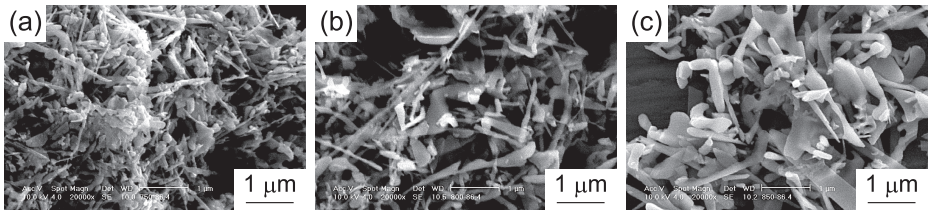

Fig. 10 Precipitates electrolytically extracted from the alloys aged at (a) 1023 K, (b) 1073 K and (c) 1123 K for 86.4 ks.

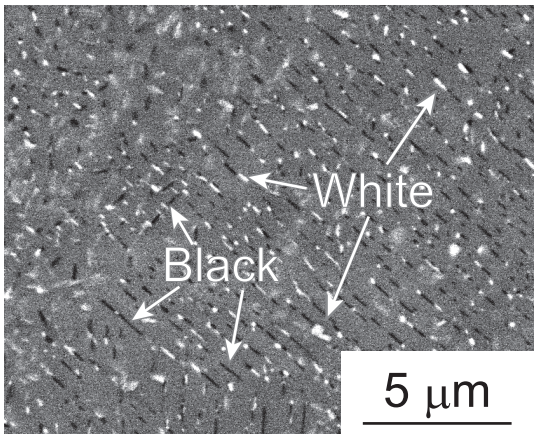

Fig. 11 SEM/BSE image of the alloy aged at 1073 K for 86.4 ks.

1123 K are larger than those at 1023 and 1073 K. In addition, the precipitated areas in the alloys aged at 1023 K for 86.4 ks and at 1073 K for 32.6–86.4 ks are much larger than those formed under other conditions (Fig. 4). Wide-area precipitation and the formation of fine precipitates appear to be the source of the increase in hardness during aging. The conditions under which this increase is observed (Fig. 9) are similar to those under which the formation of the ε-phase is detected (Fig. 8). The ε-phase formation would contribute to the increased hardness of the aged alloy.

Figure 11 shows an SEM/backscattered electron (BSE) image of the alloy aged at 1073 K for 86.4 ks, where a marked increase in hardness was obtained and a precipitated microstructure was observed across the entire area. Two types of precipitate, which appear as black and white in Fig. 11, are present in the aged alloy. The $M_{23}X_6$-type precipitate is a Cr-rich phase with less Mo than the η-phase and π-phase precipitates[15]. Therefore, the black precipitates in Fig. 11 seem to be $M_{23}X_6$-type. The white precipitates correspond to η-phase and π-phase precipitates. Because the precipitates are very small, their chemical compositions could not be determined using an electron-probe micro analyzer (EPMA). Determination of the phases and chemical compositions of precipitates using transmission electron microscopy is planned as future work.

4. Conclusion

Changes in the microstructures and Vickers hardness of a biomedical Co-27Cr-6Mo-0.77Si-0.64Mn-0.17N-0.06C (mass%) alloy during aging at temperatures of 973 to 1373 K for times up to 86.4 ks were investigated. The following results were obtained.

(1) The precipitates formed during aging were the η-phase, $M_{23}X_6$-type and π-phase. The η-phase and $M_{23}X_6$-type precipitates were observed between 973–1323 K and 973–1223 K, respectively. The formation of π-phase precipitates was detected in alloys aged between 1023 and 1123 K for holding times $\geq$ 21.6 ks, with a nose temperature between 1073 and 1123 K. This is the first report of the formation of π-phase precipitates during aging at low temperatures in a Co-Cr-Mo alloy system.

(2) The formation of an hcp ε-phase was observed between 1023 and 1123 K for holding times $\geq$ 32.4 ks, with a nose temperature at approximately 1073 K.

(3) At aging temperatures of 1023 and 1073 K, the hardness increased from 328 Hv to 492 and 539 Hv, respectively. The formation of π-phase and ε-phase and wide-area precipitation are the primary causes of this increased hardness.

Acknowledgments

This study was supported financially by a Grant-in-Aid for Scientific Research from the Ministry of Education, Culture, Sports, Science and Technology (MEXT), Japan, under Contract No. 25249094.

REFERENCES

1) T.M. Devine and J. Wulff: J. Biomed. Mater. Res. **9** (1975) 151–167.
2) M. Niinomi, T. Hanawa and T. Narushima: JOM **57**[4] (2005) 18–24.
3) T. Narushima, K. Ueda and Alfirano: Co-Cr Alloys as Effective Metallic Biomaterials, in Advanced in Metallic Biomaterials: Tissues, Materials and Biological Reactions, edited by M. Niinomi, T. Narushima and M. Nakai (Springer, 2015), pp. 157–178.
4) H.S. Dobbs and J.L.M. Robertson: J. Mater. Sci. **18** (1983) 391–401.
5) M. Gómez, H. Mancha, A. Salinas, J.L. Rodríguez, J. Escobedo, M. Castro and M. Méndez: J. Biomed. Mater. Res. **34** (1997) 157–163.
6) A. Chiba, K. Kumagai, N. Nomura and S. Miyakawa: Acta Mater. **55** (2007) 1309–1318.
7) Y. Chen, Y. Li, S. Kurosu, K. Yamanaka, N. Tang, Y. Koizumi and A. Chiba: Wear **310** (2014) 51–62.
8) Y. Chen, Y. Li, S. Kurosu, K. Yamanaka, N. Tang and A. Chiba: Wear **319** (2014) 200–210.
9) S. Mineta, S. Namba, T. Yoneda, K. Ueda and T. Narushima: Metall. Mater. Trans. A **41** (2010) 2129–2138.
10) Alfirano, S. Mineta, S. Namba, T. Yoneda, K. Ueda and T. Narushima: Metall. Mater. Trans. A **42**(2011) 1941–1949.
11) Alfirano, S. Mineta, S. Namba, T. Yoneda, K. Ueda and T. Narushima: Metall. Mater. Trans. A **43** (2012) 2125–2132.
12) S. Mineta, Alfirano, S. Namba, T. Yoneda, K. Ueda and T. Narushima: Metall. Mater. Trans. A **43** (2012) 3351–3358.
13) S. Mineta, Alfirano, S. Namba, T. Yoneda, K. Ueda and T. Narushima: Metall. Mater. Trans. A **44** (2013) 494–503.
14) K. Sugawara, Alfirano, S. Mineta, K. Ueda and T. Narushima: Metall.

Mater. Trans. A **46** (2015) 4342–4350.
15) T. Narushima, S. Mineta, Y. Kurihara and K. Ueda: JOM **65** (2013) 489–504.
16) J.W. Weeton and R.A. Signorelli: Trans. Am. Soc. Met. **47** (1955) 815–852.
17) R.N.J. Taylor and R.B. Waterhouse: J. Mater. Sci. **18** (1983) 3265–3280.
18) R.N.J. Taylor and R.B. Waterhouse: J. Mater. Sci. **21** (1986) 1990–1996.
19) C. Montero-Ocampo, M. Talavera and H. Lopez: Metall. Mater. Trans. A **30** (1999) 611–620.
20) A. Chiba, S.-H. Lee, H. Matsumoto and M. Nakamura: Mater. Sci. Eng. A **513–514** (2009) 286–293.
21) M. Mori, K. Yamanaka, H. Matsumoto and A. Chiba: Mater. Sci. Eng. A **528** (2010) 614–621.
22) A.J. Dempsey, R.M. Pilliar, G.C. Weatherly and T. Kilner: J. Mater. Sci. **22** (1987) 575–580.
23) K. Yamanaka, M. Mori and A. Chiba: J. Mech. Behav. Biomed. Mater. **29** (2014) 417–426.
24) S. Kurosu, H. Matsumoto and A. Chiba: Mater. Lett. **64** (2010) 49–52.
25) R. Varano, J.D. Bobyn, J.B. Medley and S. Yue: Proc. IMechE H: JEIM, **220** (2006) 145–159.
26) M. Sage and C. Guillaud: Rev. Metall. **47** (1950) 139–145.
27) P. Olier, F. Barcelo, J.L. Bechade, J.C. Brachet, E. Lefevre and G. Guenin: J. Phys. IV France **7** (1997) C5-143–C5-148.
28) S. Kurosu, N. Nomura and A. Chiba: Mater. Trans. **48** (2007) 1517–1522.
29) S. Kurosu, H. Matsumoto and A. Chiba: Metall. Mater. Trans. A **41** (2010) 2613–2625.
30) Alfirano, S. Mineta, S. Namba, T. Yoneda, K. Ueda and T. Narushima: Mater. Sci. Forum, **654–656** (2010) 2180–2183.
31) H.F. López and A.J. Saldivar-Garcia: Metall. Mater. Trans. A **39** (2008) 8–18.
32) A.J. Saldívar García, A.M. Medrano and A.S. Rodríguez: Metall. Mater. Trans. A **30** (1999) 1177–1184.